สำนักงานวิทยทรัพยากร
จุฬาลงกรณ์มหาวิทยาลัย

CHAPTER IV

SUPRAMOLECULAR POLYMERIZATION OF BENZOXAZINE DIMER DERIVATIVES VIA HYDROGEN BOND AND METAL ION COMPLEXATION SYSTEM

4.1 Abstract

A novel benzoxazine-based hydrogen bond network and metallo-supramolecule are proposed. Diamine-linked benzoxazine dimers prepared by the ring opening reaction of diamine-based benzoxazine monomers are good models for supramolecular assembly via hydrogen bonding and metal ion complexation. By adding metal salt, e.g. $CuCl_2$, $Cu(ClO_4)_2$, and $CuSO_4$, the diamine-linked benzoxazine dimers shows a bathochromic effect with a new peak at 313 nm and takes maximum when the metal-dimer ratio is equal to 1:1. At this ratio, the complex also shows an increase in hydrodynamic radius as evaluated by DLS technique. An increase in viscosity as well as the change of morphology from spherical shape to rod-like shape as seen in SEM and TEM micrographs insists the development of benzoxazine polymeric chain based hydrogen bond network and metal ion complexation.

4.2 Introduction

In recent years there has been an enormous growth of interest in the field of supramolecular polymer (Brunsveld *et al.*, 2001), which refers to the chains of small molecules held together by weak reversible noncovalent interactions (Weng *et al.*, 2009). Self-assembled polymers can be controlled by the molecular interactions, stoichiometry, and binding kinetics of the supramolecular motif (De Greef *et al.*, 2009). The dynamic nature of supramolecular polymers shows their behavior to be influenced by external conditions, such as monomer concentration, temperature, and pressure, in the way that traditional covalent polymers are not possible. A wide range of noncovalent interaction, such as hydrophobic interactions (Kastner, 2001), π–π

stacking (Lehn, 1995), hydrogen bonding (Kiezer *et al.*, 2003), and metal-ligand interations (Hinderberger *et al.*, 2004) is known to induce supramolecular polymers.

For the past few years, our group has focused on *N,N*-bis(2-hydroxyalkylbenzyl)alkylamine since its advantages of simple preparation and high reaction yield (Laobuthee *et al.*, 2001, 2003; Phongtamrug *et al.*, 2004, 2005, 2006). These derivatives were obtained by a single ring opening reaction of benzoxazine derivatives with phenol compounds. The single crystallography analysis pointed out that the derivatives were in a unique structure with inter- and intramolecular hydrogen bond networks to provide asymmetric compounds (Laobuthee *et al.*, 2001). Our work also extended to the supramolecular chemistry of *N,N*-bis(2-hydroxyalkylbenzyl)alkylamine by showing how these derivatives can be host molecules to accept various guest species such as alkali, alkaline earth, and transition metal ions (Laobuthee *et al.*, 2003; Phongtamrug *et al.*, 2004).

As benzoxazine dimers accept metal ions as guests, the growth of benzoxazine dimer to polymeric chain via metal-ligand interactions can be expected. The present work, thus, is another supramolecular study to develop a novel type of bifunctional benzoxazine supramolecules, so-called benzoxazine metallo-supramolecular polymer, based on diamine-linked benzoxazine dimers. Herein, a metallo-supramolecular polymer of benzoxazine dimers is proven by various analytical techniques such as UV-Vis, DLS, NMR, including morphological analyses by SEM and TEM.

4.3 Experimental

Materials

Paraformaldehyde, 2,4-dimethylphenol, and cupric acetate monohydrate were purchased from Fluka, Switzerland. Sodium hydroxide and isopropanol were obtained from Carlo Erba, Italy. Ethylenediamine and copper (II) sulfate pentahydrate were purchased from Sigma-Aldrich, Germany. Copper (II) perchlorate

hexahydrate was obtained from Aldrich, Germany. Cupric chloride dehydrate was received from Shimakyu's Pure Chemical, Japan. Chloroform, acetonitrile, diethylether, methanol, and *t*-butanol were provided from Labscan, Ireland. Deuterated chloroform, deuterated dimethylsulfoxide, and deuterated acetonitrile were obtained from Aldrich, Germany. All chemicals were used as received.

Instruments and Equipment

Fourier transform infrared spectra (FTIR) were recorded by a Nicolet Nexus 670 FT-IR spectrometer in the range 4000-400 cm^{-1}. ^1H NMR was obtained from a Bruker ultrashield plus 500 MHz NMR spectrometer. Mass spectroscopy was analyzed by a Bruker a micrOTOF II electrospray ionization mass spectrometer (ESI-MS) and a Bruker Autoflex III Matrix-assisted laser desorption/ionization-time of flight mass spectrometer (MALDI-TOF). Particles size was measured by a Malvern zetasizer (nano-ZS). Specific viscosity was evaluated by a CANNON ubbelohde 50 B582 with a constant temperature bath CANNON CT1000. Absorption of compounds and kinetic of reaction were gained from a Shimadzu UV-Vis spectrophotometer (UV-1800). Morphology of supramolecular polymers was captured by a Hitachi H-7650 transmission electron microscope (TEM) and a Hitachi S-4800 ultra-high resolution cold field emission scanning electron microscope (FE-SEM).

Synthesis

Bifunctional Benzoxazine Derivatives

Compound **1** was prepared as reported elsewhere (Laobuthee *et al*, 2001). In brief, 2,4-dimethylphenol (12.207 g, 100 mmol), paraformaldehyde (6.302 g, 210 mmol) and ethylenediamine (3.343 ml, 50 mmol) in chloroform (15 ml) were stired at 70°C until the light yellow viscous solution was obtained. The crude product was washed by 1 M sodium hydroxide and water several times and recrystallized in a

mixed solvent of chloroform and methanol (1:1, v/v). The white crystals were dried to yield 86%.^{1}H NMR (500 MHz, $CDCl_3$): δ 6.84 (2H, s), 6.64 (2H, s), 4.93 (2H, s), 4.03 (4H, s), 3.00 (4H, s), 2.25 (6H, s), 2.18 (6H, s). ESI-MS: *m/z* 353.22 $[M+H]^+$.

Compound **2** was accomplished by the ring opening reaction as reported previously (Laobuthee *et al.*, 2001). In brief, 2,4-dimethylphenol (12.207 g, 100 mmol), was added into **1** (17.600 g, 50 mmol) in chloroform (15 ml) and allowed stirring at 120°C until the yellow viscous solution was obtained. The crude product was further purified in a mixed solvent of chloroform and methanol (1:1 v/v). The white crystals were dried to yield **2** for 80%. ^{1}H NMR (500 MHz, $CDCl_3$): δ 6.86 (4H, s), 6.67 (4H, s), 3.60 (8H, s), 2.77 (4H, s), 2.22 (12H, s), 2.19 (12H, s). ESI-MS: *m/z* 597.37 $[M+H]^+$.

Compound **3** was prepared as reported elsewhere (Laobuthee *et al*, 2001). In brief, 2,4-dimethylphenol (12.207 g, 100 mmol), paraformaldehyde (6.302 g, 210 mmol) and hexamethylenediamine (3.343 ml, 50 mmol) in chloroform (15 ml) were stirred at 70°C until the light yellow viscous solution was obtained. The crude product was washed by 1 M sodium hydroxide and water several times and recrystallized in a mixed solvent of chloroform and methanol (1:1 v/v). The white crystals were dried to yield 80%. ^{1}H NMR (500 MHz, $CDCl_3$): δ 6.86 (4H, s), 6.67 (4H, s), 3.60 (8H, s), 2.77 (4H, s), 2.22 (12H, s), 2.19 (12H, s). ESI-MS: *m/z* 408.58 $[M+H]^+$.

Compound **4** was accomplished by the ring opening reaction as reported previously (Laobuthee *et al.*, 2001). In brief, 2,4-dimethylphenol (12.207 g, 100 mmol), was added into **1** (17.600 g, 50 mmol) in chloroform (15 ml) and allowed stirring at 120°C until the yellowwish viscous solution was obtained. The crude product was further purified in a mixed solvent of chloroform and methanol (1:1 v/v). The white crystals were dried to yield **4** for 87%. ^{1}H NMR (500 MHz, $CDCl_3$): δ 6.88 (4H, s), 6.73 (4H, s), 3.73 (8H, s), 2.55 (4H, t, *J*=6.5 Hz), 2.24 (24H, s), 2.62 (4H, m), 1.22 (4H, m). ESI-MS: *m/z* 653.43 $[M+H]^+$.

Scheme 4.1 Synthesis of bifunctional benzoxazine derivatives.

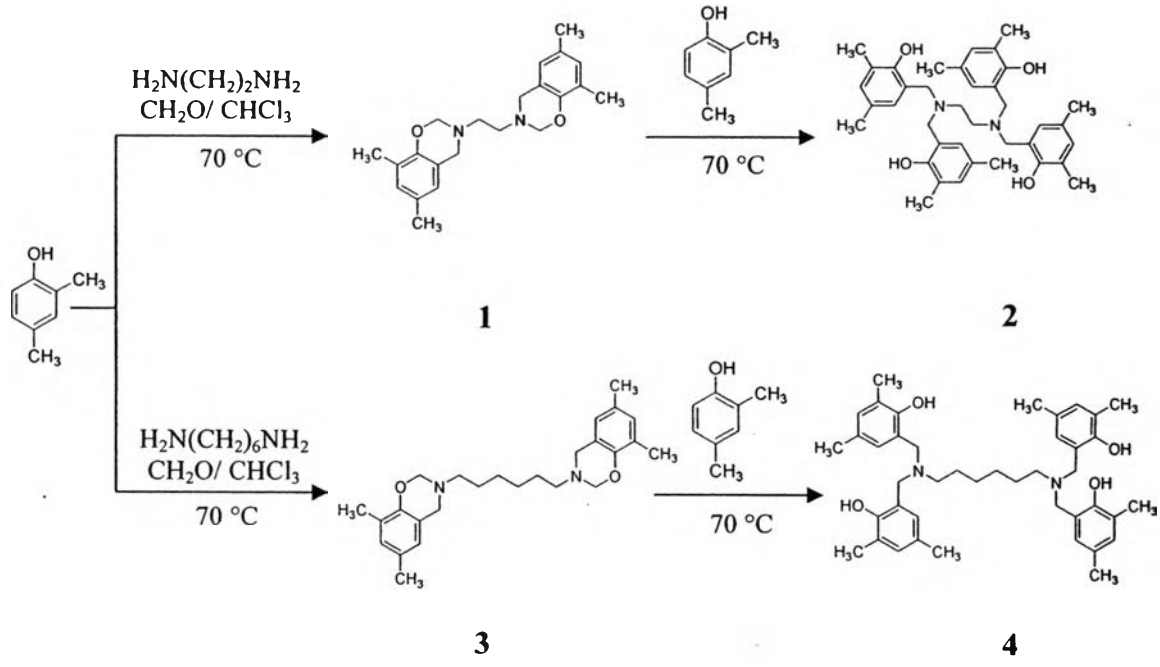

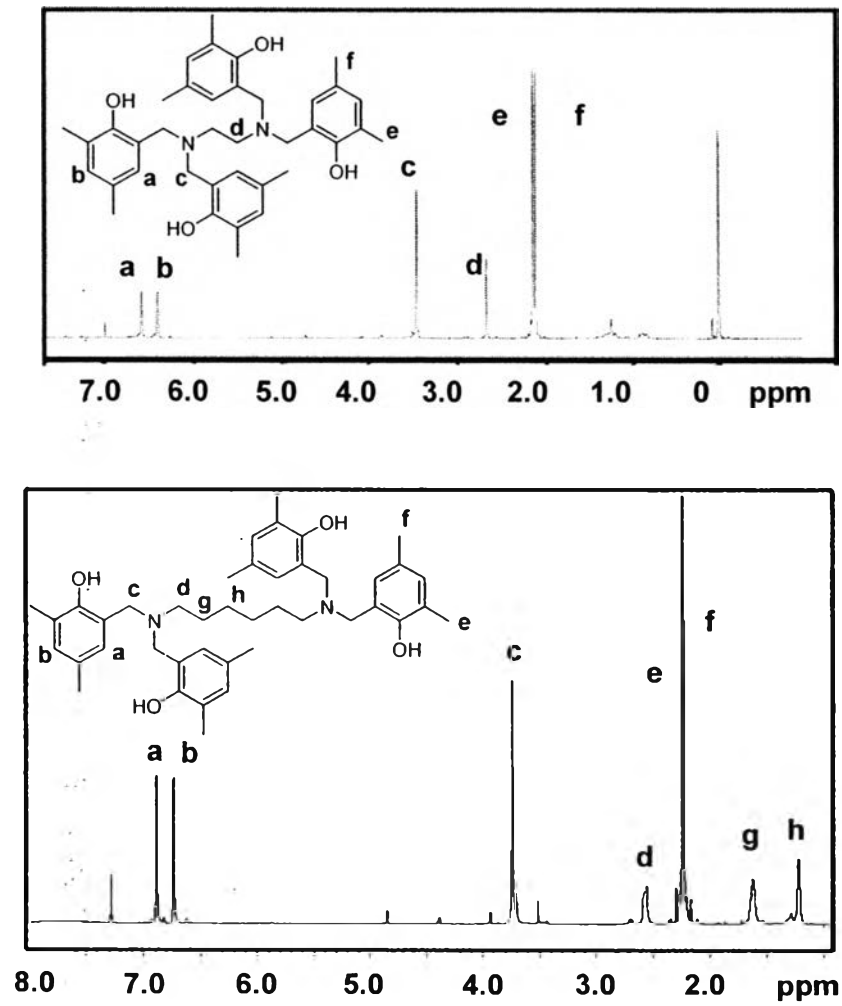

Figure 4.1 ^{1}H NMR spectra of **2** and **4** in $CDCl_3$ at 500 MHz.

Preparation of Metallo-supramolecular System

A solution containing 29.85 mg (0.05 mmol) of **2** in DMSO (1 ml) was mixed with a stoichiometric amount of 18.53 mg (0.05 mmol) of copper (II) perchlorate hexahydrate in DMSO (1 ml). Other copper salts, i.e., cupric acetate monohydrate, copper (II) sulfate pentahydrate and cupric chloride dehydrate were used to prepare the complex with **2** in similar procedures. Compound **4** was also used to prepare similar complexation with the copper salts. The mixture was then left for 3 days before characterization.

4.4 Results and discussion

Benzoxazine Supramolecular Polymer via Metal Ion Complexation

Self Assembly and Solution Properties of the Metallo-supramolecular Polymer

The supramolecular performance of benzoxazine dimers, **2** and **4**, was studied based on the complexation with various types of copper salts, i.e., $CuCl_2$, $CuSO_4$, $Cu(ClO_4)_2$ and $Cu(CH_3COO)_2$ in DMSO solvent. Figure 4.2 shows UV spectra of **2** and **4** before and after mixing with $CuCl_2$ in DMSO. It is clear that when **2** and **4** form the complex with copper, new peaks at 342 nm and 353 nm are observed. It is important to note that the new peaks observed were differed based on the type of copper salts. For example, in the case of the complexation with $CuCl_2$, $CuSO_4$, $Cu(ClO_4)_2$, and $Cu(CH_3COO)_2$, the new peaks are at 342 nm, 353 nm, 428 nm, and 313 nm, respectively.

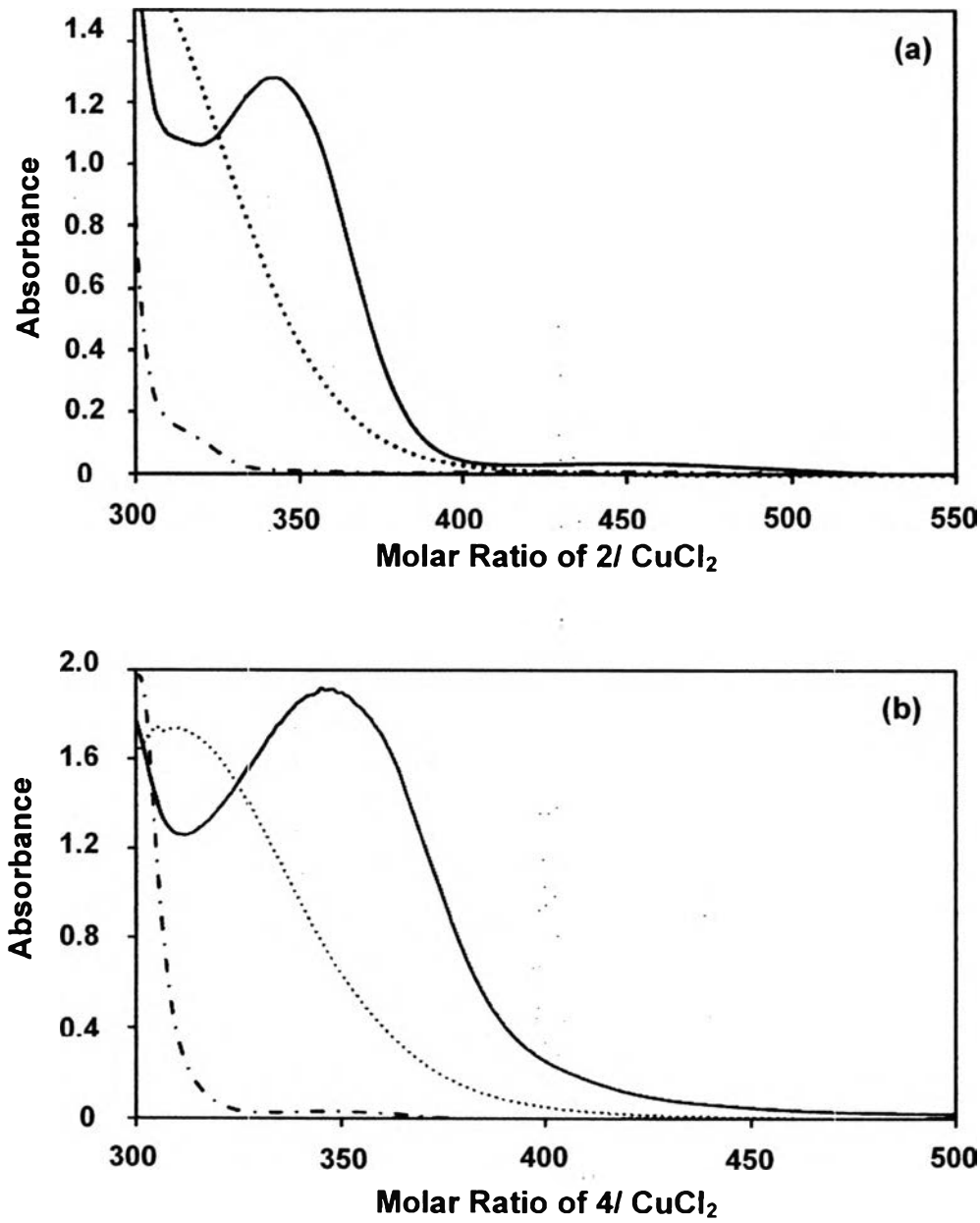

Figure 4.2 UV spectra of (a) **2** (• – • –); $CuCl_2$ (·····), and **2**/$CuCl_2$ (———) and (b) **4**(• – • –); $CuCl_2$ (·····), and **4**/$CuCl_2$ (———)

Figure 4.3 (a) is the plot of the new UV peak of each complex related to the molar ratios. It is clear that all types of copper salts show the highest absorbance at

1:1 molar ratio. In other words, the host-guest complexation between **2** and copper ion is 1:1.

In the case of **4**, the host-guest complexation is different from that of **2**. As indicated in Figure 4.2 (b), the host-guest ratio is depending on the type of the metal ion. Only **4**/$CuSO_4$; the host-guest ratio is 1:1, whereas those of **4**/$CuCl_2$ and **4**/$Cu(ClO_4)_2$; the host-guest ratio are 5:1 and that of **4**/$Cu(CH_3COO)_2$; the host guest ratio is 1:2. It is not yet clear about the structure of the 5:1 host-guest ratio, however, in the past, there were some reports similar to these cases (Rohacova *et al.*, 2010).

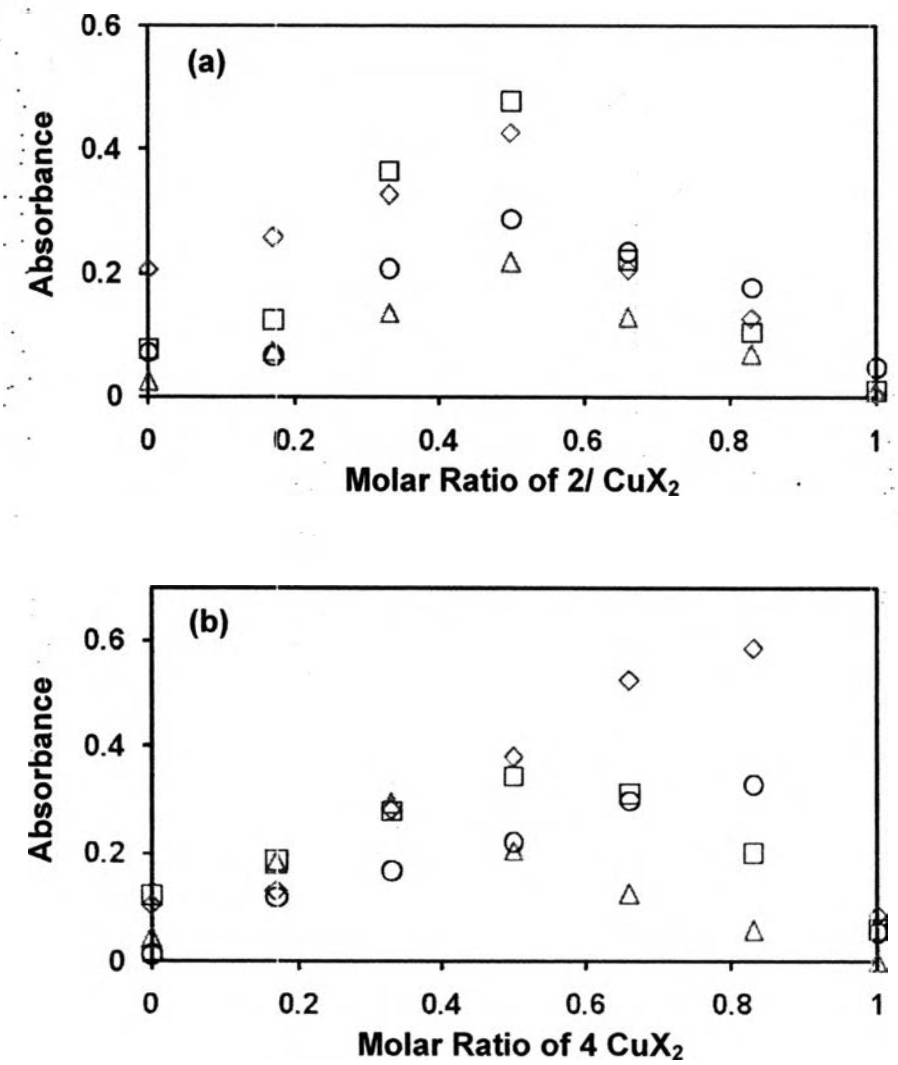

Figure 4.3 (a) UV spectra of **2**/CuX_2 at different molar ratios in DMSO, and (b) UV spectra of **4**/CuX_2 at different molar ratios in DMSO (◇: $CuCl_2$, ○: $Cu(ClO_4)_2$, □: $CuSO_4$, and △: $Cu(CH_3COO)_2$.

Specific viscosity and molecular assembly size (particle size) are other information to confirm the supramolecular polymer formation. In 2003 Beck *et al.* reported an increase in viscosity related to the host-guest formation of 2,6-bis(1'-methylbenzimidazolyl)pyridine-terminated monomers with metal ions system. Figure 4.4 shows the specific viscosity of **2** after complexation with various types of copper salts. It is clear that all complexes show an increase in viscosity related to the amount of **2**. Although it is expected to see the highest viscosity at 1:1 host-guest ratio, only **2**/$Cu(ClO_4)_2$ shows the highest viscosity at 1:1 ratio whereas other complexes are fluctuated.

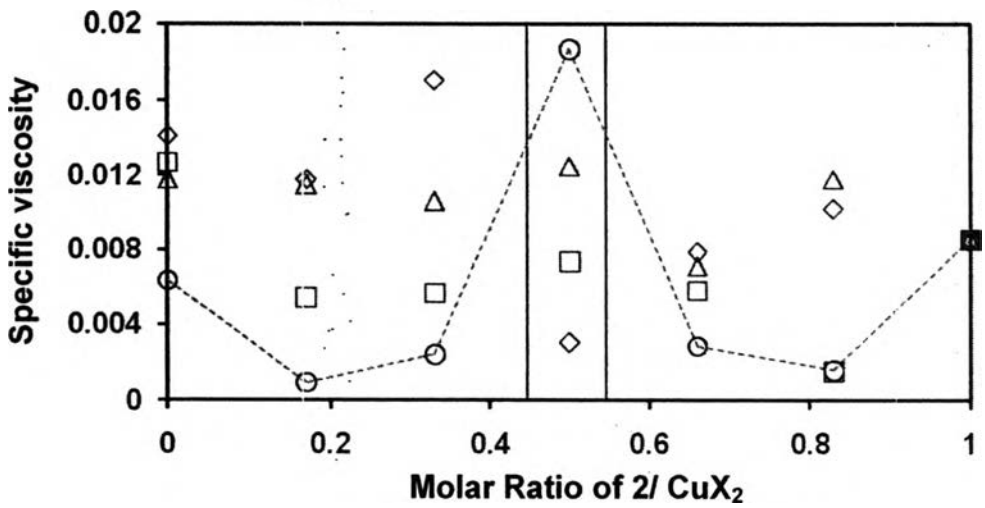

Figure 4.4 Specific viscosity of **2**/CuX_2 at different molar ratios in DMSO (◇: $CuCl_2$, ○: $Cu(ClO_4)_2$, □: $CuSO_4$, and △: $C_4H_6CuO_2$).

Figure 4.5 shows the average particle sizes of **2** and **4** after complexation with $Cu(ClO_4)_2$. It is clear that the particle size of **2**/$Cu(ClO_4)_2$ becomes as high as 380 nm when the host-guest ratio is 1:1. This implies that **2**/$Cu(ClO_4)_2$ might form a stable metallo-supramolecular polymer.

As **2** and $Cu(ClO_4)_2$ might be a good model to show the formation of metallo-polymer system as evidenced from the saturation of hyperchromic effect at 313 nm for 1:1 molar ratio (Figure 4.6). The metallo-supramolecular formation evaluated from the repeating units of supramolecular polymer was studied by using ^1H NMR end-group analysis. At 1:1 molar ratio, concentration 0.005 M, the end-group

analysis by ^{1}H NMR confirms the repeating unit to be 4 as shown in the calculation (Figure 4.7).

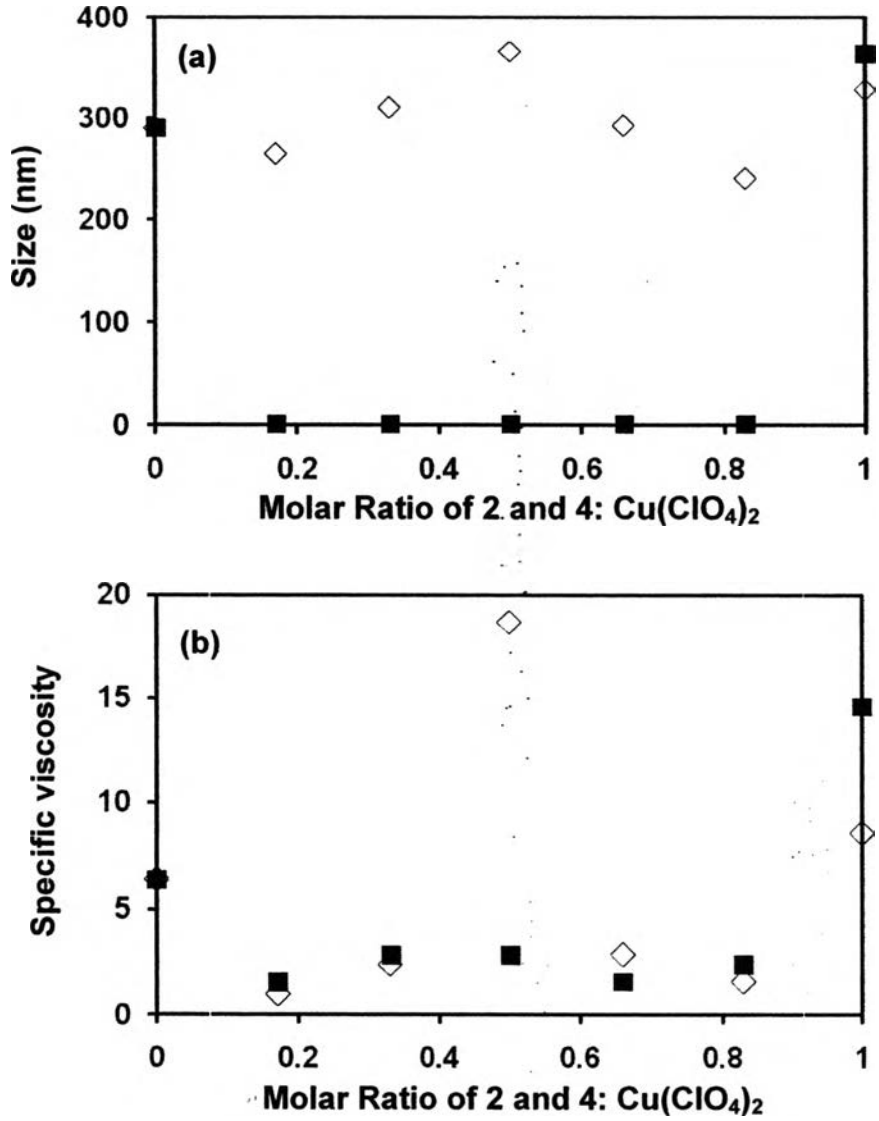

Figure 4.5 (a) Size of **2**: $Cu(ClO_4)_2$ (◇, nm) and **4**: $Cu(ClO_4)_2$ (■, nm) at different molar ratios in DMSO, and (b) specific viscosity of **2**: $Cu(ClO_4)_2$ (◇) and **4**: $Cu(ClO_4)_2$ (■) at different molar ratios in DMSO.

Metallo-supramolecular polymer in solution system can also be evaluated by specific viscosity. Figure 4.8 shows plot of specific viscosity and plot of particle size related to the concentration of the metal complex of **2** and **4**. An increase in size of

the supramolecular polymer as a function of concentration was verified by dynamic light scattering (DLS) technique to find a gradual increase in specific viscosity with an increase in complex $[\mathbf{2}\cdot Cu(ClO_4)_2]_n$ concentration. A linear relationship (slope~1.213) indicates the presence of noninteracting species and no aggregation behavior in this system. This result is relevant to the report by Beck *et al.* (2003) and confirms our case to be a metallo-supramolecular system.

Morphology of Metallo-supramolecular Polymer.

It comes to our question whether the supramolecular structured **2** and Cu^{2+} brings any changes in morphology. The morphology was clarified by using SEM and TEM. The spherical shape and donut shape were observed from starting material, **2**. Surprisingly, after adding an mole equivalence of $Cu(ClO_4)_2$, **2** shows the needle-like shape morphology (Figure 4.9 (a), (b), and (c)). The image from SEM (Figure 4.9(d)) also indicates the chains developed from **2**.

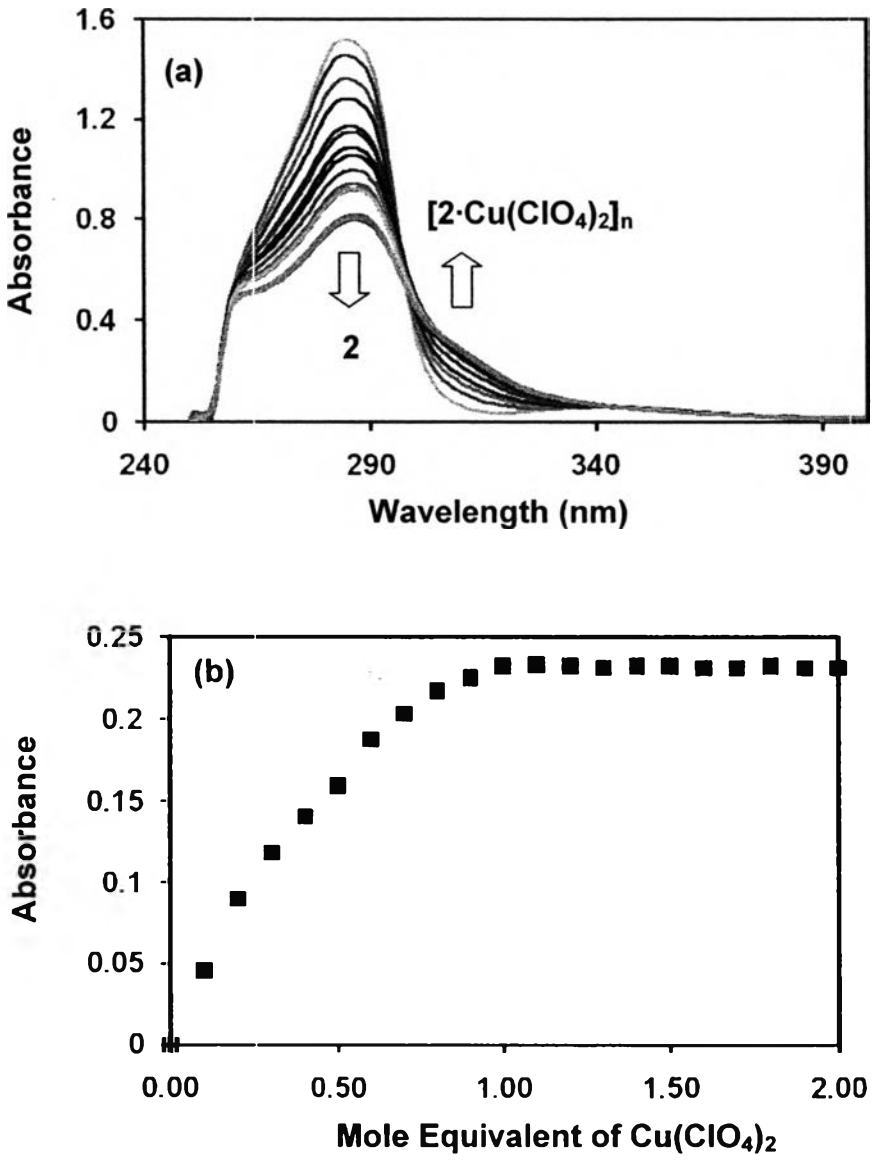

Figure 4.6 (a) UV spectra of $Cu(ClO_4)_2$: **2** at different molar ratios in DMSO, and (b) the absorbance at 313 nm obtained from various molar ratios.

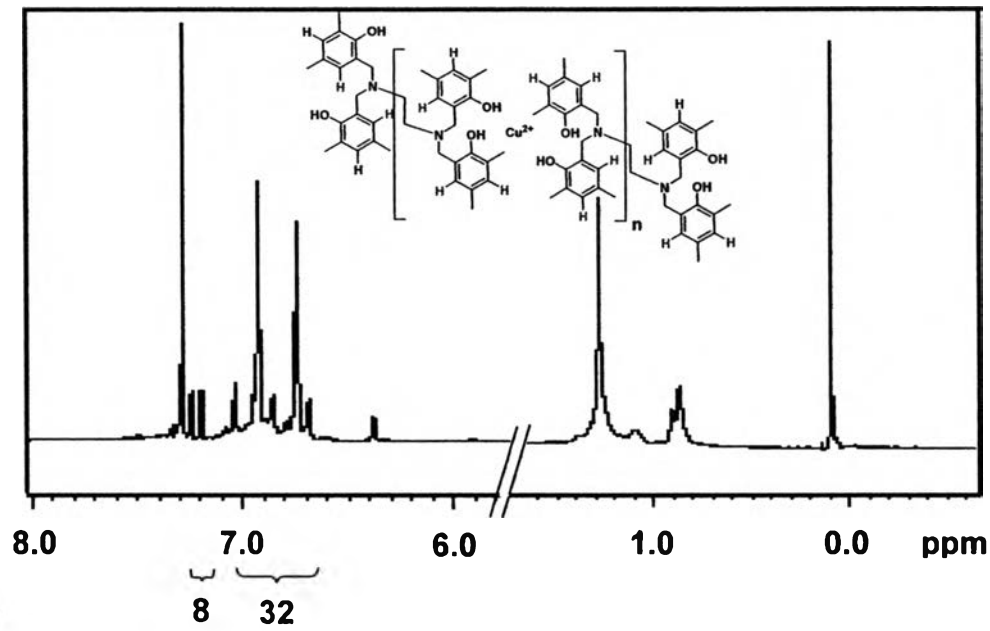

Chain Length (n) Calculation	
Only 1 repeating unit: $H_{aromatic}$	= 8
Number of repeating unit (n): n	= 32/8
	= 4

Figure 4.7 ^{1}H NMR spectrum of $[\mathbf{2}\cdot Cu(ClO_4)_2]_n$ and integral ratio for chain length calculation.

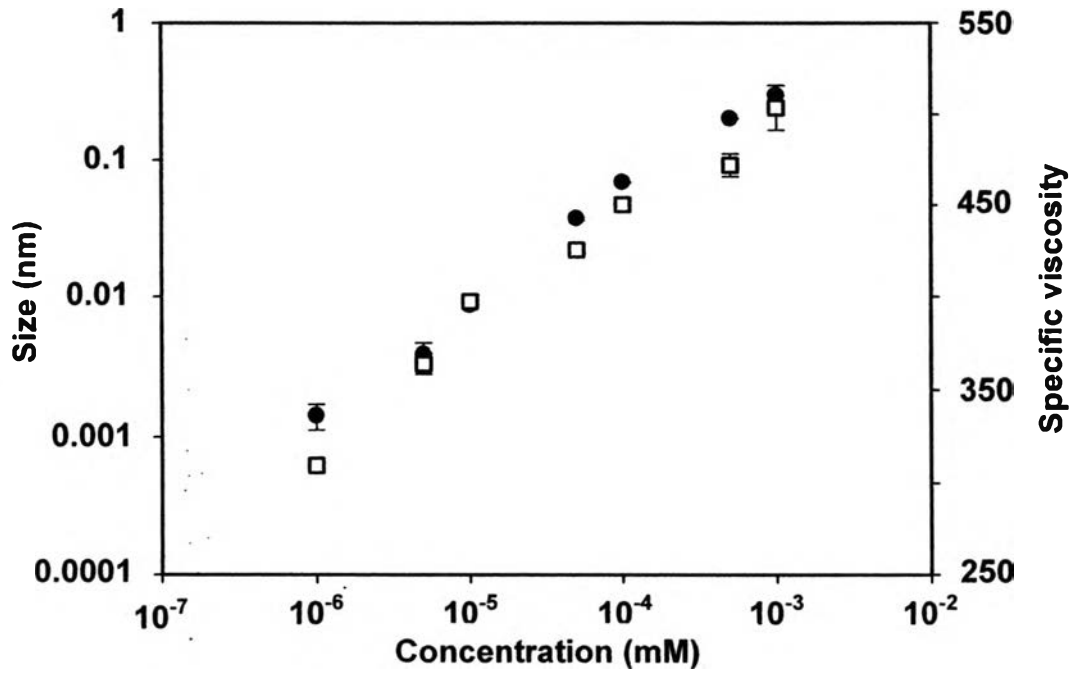

Figure 4.8 Particle size (□, nm) and specific viscosity (●) related to the concentration of $[\mathbf{2}\cdot Cu(ClO_4)_2]_n$.

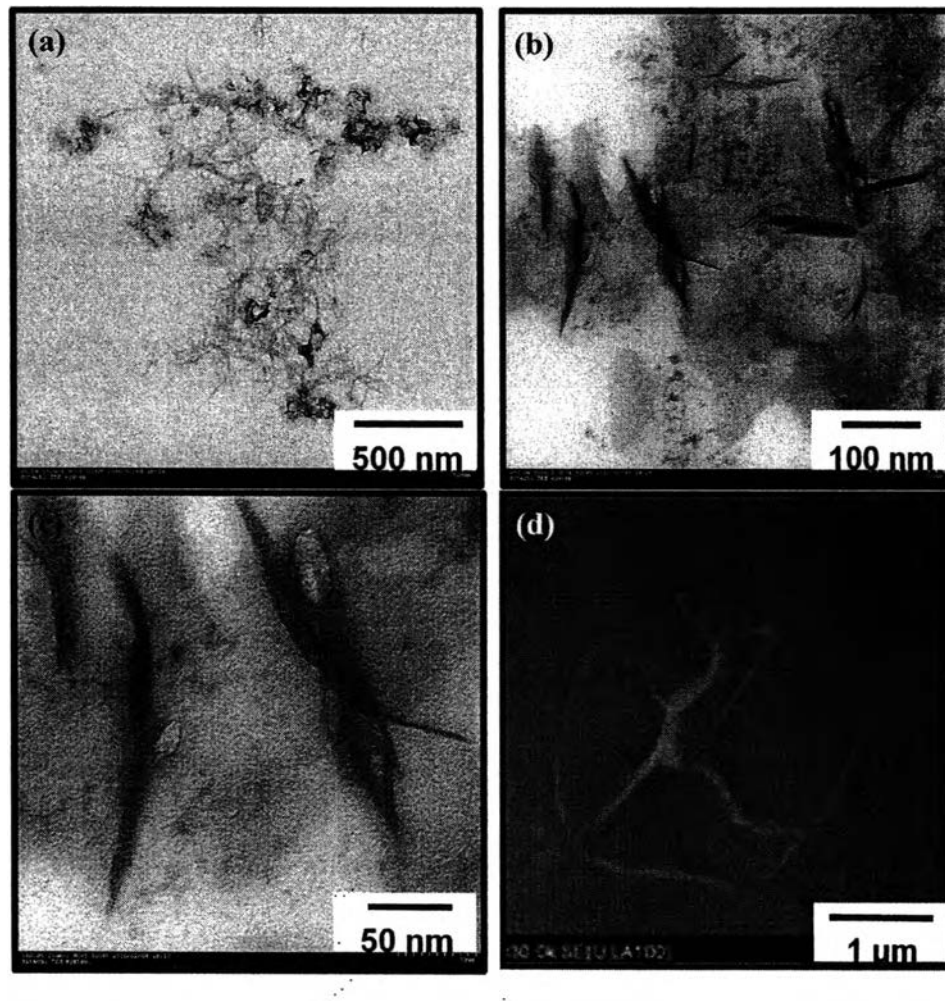

Figure 4.9 TEM micrographs of $[\mathbf{2}\cdot Cu(ClO_4)_2]_n$ at; (a) 10 k, (b) 30 k, (c) 60 k magnification, and (d) SEM micrograph of $[\mathbf{2}\cdot Cu(ClO_4)_2]_n$ at 30 k magnification.

Benzoxazine Supramolecular Polymer via Hydrogen Bond Network.

Self Assembly and Solution Properties of Benzoxazine Supramolecular Polymer.

In general, the evidences to prove hydrogen-bonded supramolecular polymer are, for example, viscosity, end group number, radius of gyration, including X-ray single crystal structure. One of characteristic properties of polymeric structures is their relatively high solution viscosity.

In 2004, ten Cate *et al.* reported specific viscosities of bifunctional 2-ureido-4[1H]-pyrimidinone (UPy) derivatives in chloroform as a function of concentration. Toward low concentration, all curves approach a slope of around 1, demonstrating a linear relation between specific viscosity and concentration, which is characteristic for non-interacting assemblies of constant size. These results confirm the presence of oligomer and cyclic dimers in dilute solution. Upon an increase in the concentration, a sharp rise in the viscosity with the slopes of 2.8-3.0 was observed. They concluded the formation of entangled polymers upon the size increasing. In our case, Figure 4.10 is a plot of specific viscosity and particle size of **2** and **4** obtained from ubbelohde viscosity measurement and dynamic light scattering techniques. It should be noted that the specific viscosities of **2** and **4** are increased as the concentration increased which slope around 1, so **2** and **4** systems might form a hydrogen bond network between molecules without aggregation and chain entanglement to give hydrogen bonded supramolecule.

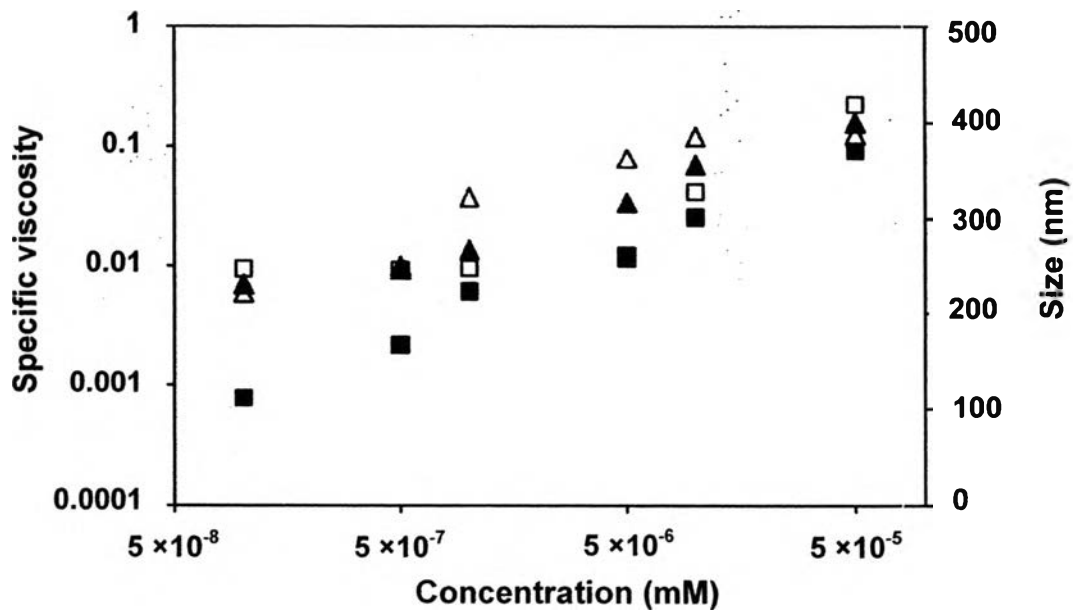

Figure 4.10 Specific viscosity (■) and particle size (□, nm) related to the concentration of **2**, and specific viscosity (▲) and particle size (△, nm) related to the concentration of **4** (303 K).

Another attempt to clarify the hydrogen bonded supramolecular system of **2** and **4** was further carried out. Spin-lattice relaxation (T1 relaxation) is a process of energy exchange between individual nuclear spins and the surrounding liquid or solid lattice. When molecules interact with each other, the interaction induces some changes to the T1 relaxation time of the molecule. The T1 is an average of the T1 values of those nuclei associated with binding and those unassociated with the site. As bound sites have a shorter relaxation time than the nonbound sites (Jayasundera, *et al.*, 2003), the T1 value is useful to evaluate how the molecule is under a specific network. Here, by simply varying the concentration of **2** and **4**, T1 value of each proton would be indirect information to let us know how the molecules are packed in hydrogen bond network to initiate supramolecular structure by observing the changes of the T1 value of each proton after the concentrations of **2** and **4** were varied (Figure 4.11). For **2** (Figure 4.11 (a)), each proton at δ=6.76, 6.63, 3.53, 2.11, and 2.62 ppm (see Figure 4.1 for characterization of **2**) do not significantly change with the concentration. This implies the hydrogen bond network of **2** may not be stable enough to increase gradually as the concentration.

In the case of **4** (Figure 4.11 (b)), the proton positions at δ=6.77, 6.70, 3.57, 2.33, 2.14, 1.43, and 1.04 ppm are gradually decreased as concentration increases. This implies that **4** might be in a tight environment when the concentration was increased. As benzoxazine dimers are in hydrogen bonded network, the decrease of T1 values related to the concentration implies the consequent hydrogen bond network.

Although the direct evidence based on the crystallography analysis might be the most reliable to confirm the hydrogen bonded supramolecular polymer of **2** and **4**, here, the T1 values suggest a stable hydrogen bonded supramolecular structure of **4**.

It comes to our question whether the hydrogen bonded supramolecular structures of **2** and **4** bring any changes in morphology. The morphologies of **2** and **4** were traced by using SEM and TEM. The samples were prepared by dissolving **2** and **4** in DMSO at the concentration of 0.005 M. It is important to note that **2** does not give any observable crystal but after dispersing on TEM sample holders, tiny crystals which can be seen by TEM were developed. As shown in Figure 4.12 (a), **2** shows

shows the donut-like morphology with a diameter of 430 nm. The donut-like morphology retains (Figure 4.12 (b)) even a level of concentration is increased. When the concentration was increased to 0.001 M, the donut-like forms were changed to spheres (Figure 4.12 (c)). The sphere-like morphology is maintained even the concentration was kept increasing to 0.005 M (Figure 4.12 (d)).

In the case of **4**, it is important to note that after **4** was dissolved in DMSO, a quantitative amount of microcrystals were obtained. Comparing to **2**, **4** shows a single type of needle-like and comb-like morphology (Figure 4.13 (a)-(d)). This might be due to a stable hydrogen bond network formed between molecules to give a well-defined packing structure which appears to be needles. Considering this result with those of T1 values (Figure 4.11 (b)), especially at δ=1.43 ppm, which is the most significant decreased value and it is belonging to methylene proton of diamine, it is possible that the methylene proton (δ=1.43) was in a tight environment to lose its degree of freedom and become difficult to rotate around. This suggests **4** forms an intermolecular hydrogen bond network.

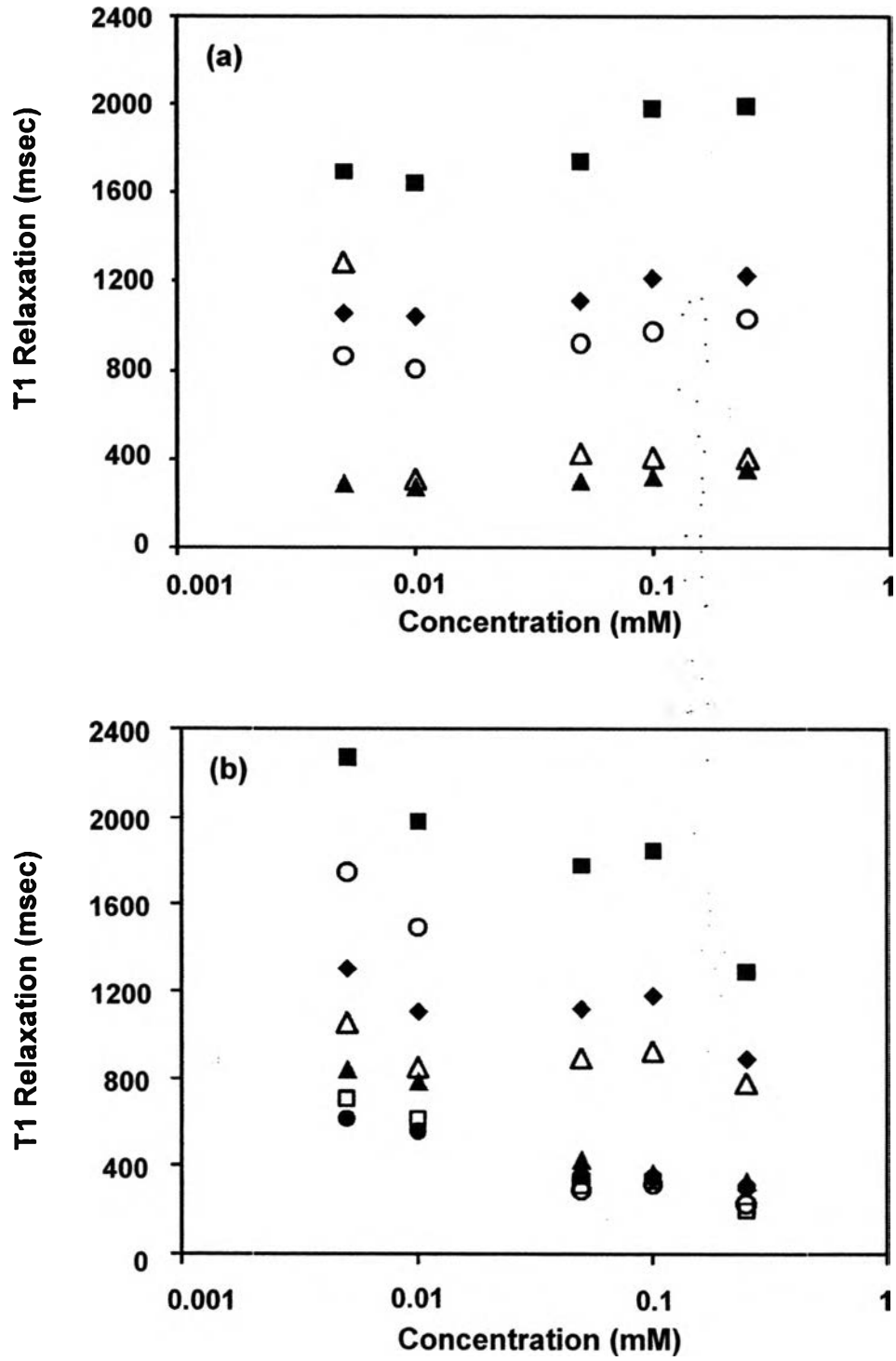

Figure 4.11 (a) T1 relaxation of each proton of **2** system with various concentrations (■; δ=6.77 ppm, ◆; δ= 6.63 ppm, △; δ= 3.53 ppm, ▲; δ= 2.62 ppm, and ○; δ= 2.11 ppm), and (b) T1 relaxation of each proton of **4** system with various

concentrations(■; δ=6.76 ppm, ◆; δ= 6.70 ppm, ▲; δ= 3.57 ppm, ●; δ= 2.33 ppm, △; δ= 2.14 ppm, ○; δ= 1.43 ppm and □; δ= 1.04 ppm).

Although **2** and **4** were different only in term of chain length of methylene in diamine unit, the decrease in T1 value and the changes in morphology related to the concentration suggest us that an appropriate chain length of methylene unit might allow an effective hydrogen bond network. Therefore, in the case of **4**, a stable supramolecular polymer under hydrogen bond network can be observed.

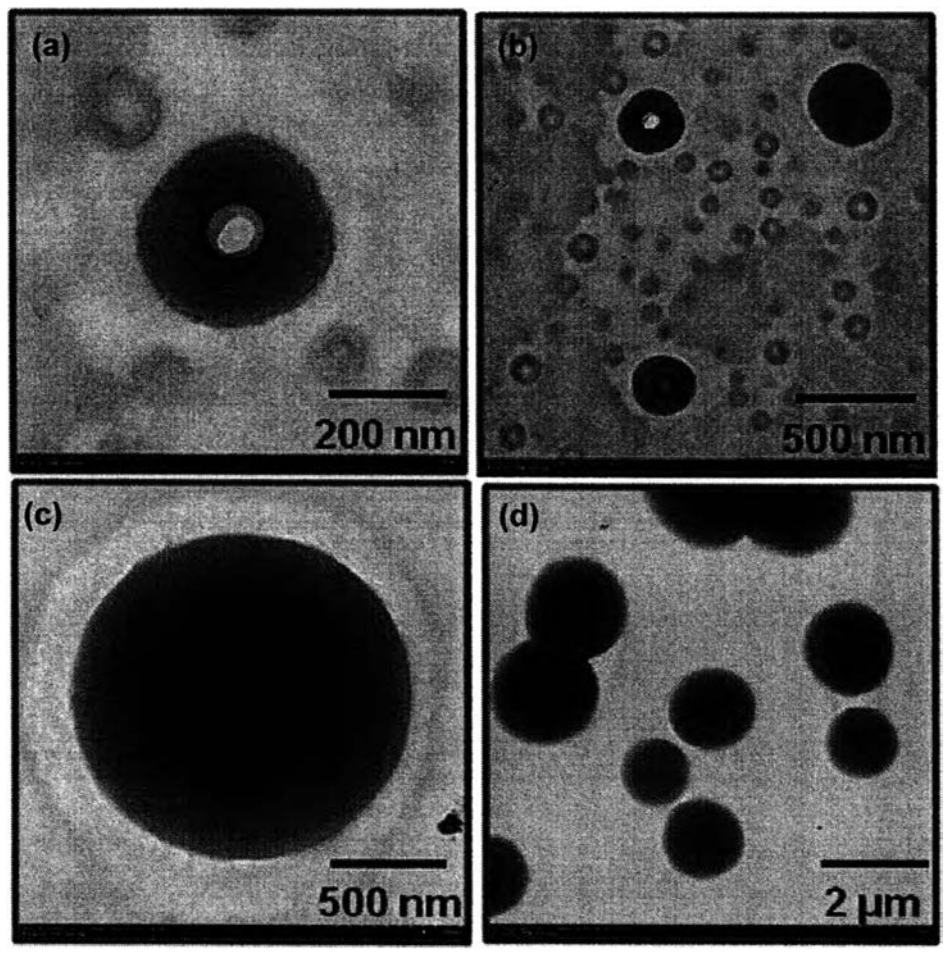

Figure 4.12 TEM micrographs of **2** system; donut shape at concentration 0.001 M; (a) 25 k and (b) 8 k magnification, and spherical shape at concentration 0.005 M; (c) 10 k and (d) 2 k magnification.

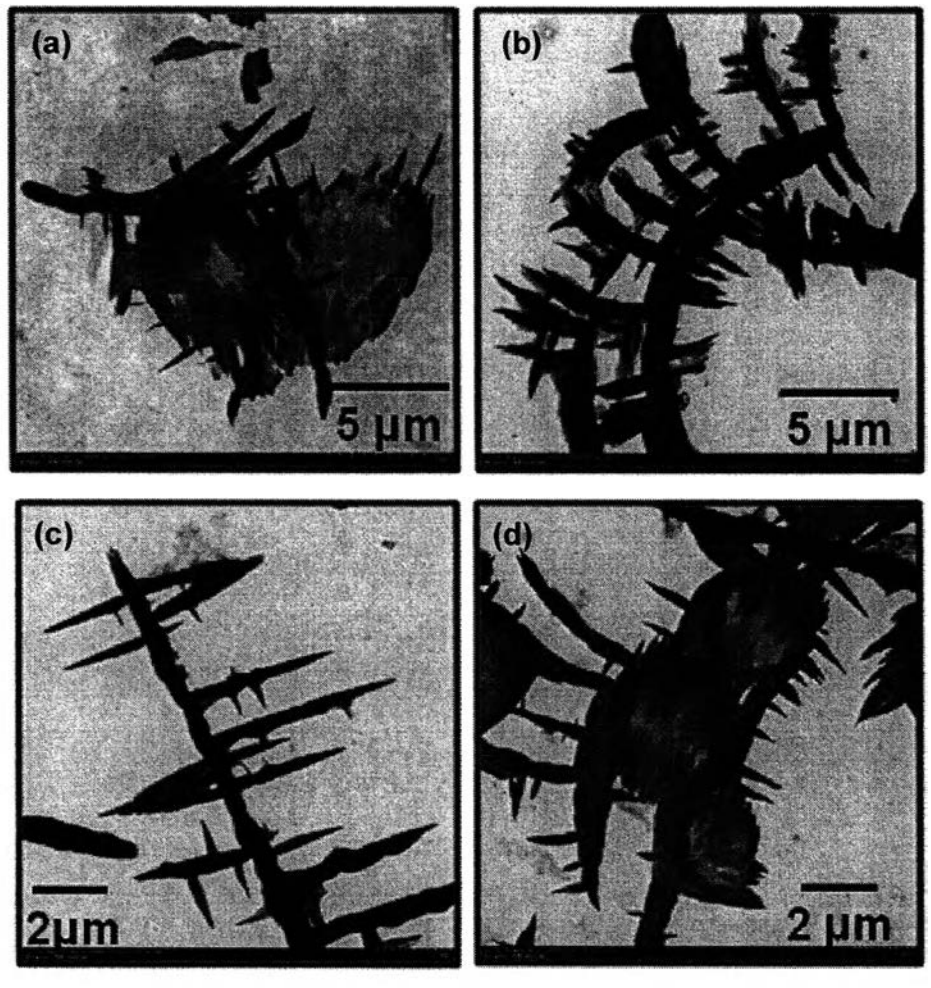

Figure 4.13 TEM micrographs of **4** system; microcrystal at; (a) 0.8 k, (b) 1 k, (c) 1.2 k, and (d) 1.5 k magnification.

Conclusions

The present work demonstrate a novel type of benzoxazine based self-assembly via hydrogen bond network and metallo-supramolecular system. In the case of metallo-supramolecular polymer, only **2** formed supramolecule via a complexation with copper (II) perchlorate. The metallo-supramolecular system showed an increase in viscosity as well as the particle size in solution state whereas it showed a needle-like morphology in solid state. For hydrogen bonded supramolecular polymer, **4** gave a stable packing structure which enabled us to confirm by the decrease in T1 value as well as the needle-like and comb-like

morphology. It is also important to note that although T1 values of **2** were maintained even the concentration increased, the morphology of **2** gradually developed from donut-like structure to sphere-like one which might be a consequence of the formation of supramolecular structure.

4.6 References

Beck, J. B., Ineman, J. M., Rowan, S. J. Macromolecules **2005**, 38, 5060-5068.

Brunsvel, L., Folmer, B. J. B., Meijer, E. W., Sijbesma, R. P. Chem. Rev. **2001**, 101, 4071-4097.

Brunworth, M., Mendez, J. D., Schroeter, M., Rowan, S. J., Weder, C. Macromolecules **2008**, 41, 2157-2163.

Chirachanchai, S., Phongtamrug, S., Rungsimanon, T. Tetrahedron Lett. **2009**, 49 (19), 181-3184.

De Greef, T. F. A., Smulders, M. M. J., Wolffs, M., Schenning, A. P. H. J., Sijbesma, R. P., Meijer, E. W. Chem. Rev. **2009**, 109, 5687-5754.

Hinderberger, D., Schmelz, O., Rehahn, M., Jeschke, G. Angew. Chem., Int. Ed. **2004**, 43, 4616-4621.

Jayasundera, S., Schmidt, W. F., Hapeman, C. J., Torrents, A. J. Agric. Food Chem., **2003**, 51, 3829–3835.

Kastner, U. Colloids Surf. A **2001**, 183-185, 805-821.

Knapton, D., Iyer, K. P., Rowan, S. J., Weder, C. Macromolecules **2006**, 39, 4069-4075.

Laobuthee, A., Chirachanchai, S., Ishida, H., Tashiro, K. J. Am. Chem. Soc. **2001**, 123, 9947-9955.

Laobuthee, A., Ishida, H., Chirachanchai, S. J. Incl. Phenom. Macrocycl. Chem. **2003**, 47, 179-185.

Lehn, M. J. **1995**, Supramolecular Chemistry: Concepts and Perspectives. Germany: VCH.

Martin, R. B. Chem. Rev. **1996**, 96, 3043-3064.

Phongtamrug, S., Chirachanchai, S., Tashiro, K. Macromol. Symp. **2006**, 242, 40-48.

Phongtamrug, S., Miyata, M., Chirachanchai, S. Chem. Lett. **2005**, 34 (5), 634-635.

Phongtamrug, S., Pulpoka, B., Chirachanchai, S. Supramol. Chem. **2004**, 16 (4), 269-278.

Phongtamrug, S., Tashiro, K., Miyata, M., Chirachanchai, S. J. Phys. Chem. B **2006**, 110, 21365-21370.

Rohacova, J., Marin M. L., Miranda, M. A. J. Phys. Chem. B **2010**, 114, 4710–4716.

Weng, W., Li, Z., Jamieson, A. M., Rowan, S. J. Macromolecules **2009**, 42, 236-246.